ELSEVIER

Chemical Engineering Journal 140 (2008) 62–70

Chemical Engineering Journal

www.elsevier.com/locate/cej

Feasibility of Na-based thermochemical cycles for the capture of CO_2 from air—Thermodynamic and thermogravimetric analyses

V. Nikulshina [a], N. Ayesa [a], M.E. Gálvez [a], A. Steinfeld [a,b,*]

[a] *Department of Mechanical and Process Engineering, ETH Zurich, 8092 Zurich, Switzerland*
[b] *Solar Technology Laboratory, Paul Scherrer Institute, CH-5232 Villigen, Switzerland*

Received 2 May 2007; received in revised form 30 July 2007; accepted 5 September 2007

Abstract

Three Na-based thermochemical cycles for capturing CO_2 from air are considered: (1) a NaOH/$NaHCO_3$/Na_2CO_3/Na_2O cycle with 4 reaction steps, (2) a NaOH/$NaHCO_3$/Na_2CO_3 cycle with 3 reactions steps, and (3) a Na_2CO_3/$NaHCO_3$ cycle with 2 reaction steps. Depending on the choice of CO_2 sorbent – NaOH or Na_2CO_3 – the cycles are closed by either $NaHCO_3$ or Na_2CO_3 decomposition, followed by hydrolysis of Na_2CO_3 or Na_2O, respectively. The temperature requirements, energy inputs, and expected products of the reaction steps were determined by thermodynamic equilibrium and energy balance computations. The total thermal energy requirement for Cycles 1, 2, and 3 are 481, 213, and 390 kJ/mol of CO_2 captured, respectively, when heat exchangers are employed to recover the sensible heat of hot streams. Isothermal and dynamic thermogravimetric runs were carried out on the pertinent carbonation, decomposition, and hydrolysis reactions. The extent of the NaOH carbonation with 500 ppm CO_2 in air at 25 °C – applied in Cycles 1 and 2 – reached 9% after 4 h, while that for the Na_2CO_3 carbonation with water-saturated air – applied in Cycle 3 – was 3.5% after 2 h. Thermal decomposition of $NaHCO_3$ – applied in all three cycles – reached completion after 3 min in the 90–200 °C range, while that of Na_2CO_3 – applied in Cycle 1 – reached completion after 15 min in the 1000–1400 °C range. The significantly slow reaction rates for the carbonation steps and, consequently, the relatively large mass flow rates required, introduce process complications in the scale-up of the reactor technology and impede the application of Na-based sorbents for capturing CO_2 from air.

Keywords: CO_2; Capture; Air; Na; NaOH; $NaHCO_3$; Solar; Thermochemical cycle

1. Introduction

In previous papers [1,2], we thermodynamically and kinetically analyzed a 3-step thermochemical cycle based on $Ca(OH)_2$–$CaCO_3$–CaO carbonation/calcination reactions for the capture of CO_2 from air. The required thermal energy input was found to be 2485 kJ/mol CO_2 captured, assuming part of the sensible heat carried by the hot CO_2-depleted air flow exiting the carbonator at 227 °C is recovered for pre-heating ambient air entering the carbonator. Ten times more energy would be required without heat recovery. The energy requirement could be reduced by making use of CO_2 sorbents that carbonate/calcine at lower temperatures but still at reasonable reaction rates. A potential candidate is NaOH, according to:

$$2NaOH(s) + CO_2(g) = Na_2CO_3(s) + H_2O(g) \qquad \Delta H^{\circ}_{298\,K} = -127.5\,kJ \tag{1}$$

$$NaOH(s) + CO_2(g) = NaHCO_3(s) \qquad \Delta H^{\circ}_{298\,K} = -131.5\,kJ \tag{2}$$

The energy requirement for a CO_2 capture process from air based on the carbonation of NaOH at ambient temperature has been estimated to be in the 0.33–0.46 MJ/mol CO_2 range [3]. The rate of CO_2 absorption into a NaOH aqueous solution was investigated at 20 °C and 8–100% CO_2 concentration [4], and in the range 0–60 °C [5,6]. Relevant experimental studies were published on the determination of the enhancement factor [7,8], the interfacial area and mass transfer coefficient [7], and the film surface temperature [9]. The CO_2 solubility was

* Corresponding author at: Department of Mechanical and Process Engineering, ETH Zurich, 8092 Zurich, Switzerland. Tel.: +41 44 6327929; fax: +41 44 6321065.
E-mail address: aldo.steinfeld@eth.ch (A. Steinfeld).

1385-8947/$ – see front matter © 2007 Elsevier B.V. All rights reserved.
doi:10.1016/j.cej.2007.09.007

given as a function of temperature and ionic strength [5], as well as of the rising speed and drag coefficient of CO_2 bubbles in a strong alkaline solution [10]. A dry sample of NaOH purged for 60 min with CO_2 at a pressure 0.08–0.12 MPa contained 100% $NaHCO_3$ [11]. Reactor concepts proposed include bubble columns [8,12,13], wetted-wall columns [14], packed columns [15,16], contactor spray-towers [17], falling films [4], and impinging jet absorbers [7].

CO_2 sorption can also be accomplished by means of Na_2CO_3, according to [18–22].

$$Na_2CO_3(s) + CO_2(g) + H_2O(g) = 2NaHCO_3(s)$$
$$\Delta H^\circ_{298\,K} = -135.5\,kJ \quad (3)$$

Depending on the choice of CO_2 sorbent – NaOH or Na_2CO_3 – the cycle can be closed either by $NaHCO_3$ decomposition (reaction (3-reverse)), or by Na_2CO_3 decomposition:

$$Na_2CO_3 = Na_2O + CO_2 \qquad \Delta H^\circ_{298\,K} = 720.7\,kJ \quad (4)$$

followed by hydrolysis of Na_2O or Na_2CO_3,

$$Na_2O + H_2O = 2NaOH \qquad \Delta H^\circ_{298\,K} = -541.3\,kJ \quad (5)$$

$$Na_2CO_3 + H_2O = 2NaOH + CO_2 \qquad \Delta H^\circ_{298\,K} = 171.5\,kJ \quad (6)$$

Na_2CO_3 was decomposed at above 800 °C with a conversion rate of 80% in 0.2 s [23,24], while the decomposition temperature could be lowered by the addition of black carbon or SiO_2 [25–27]. A kinetic model was formulated for the Na_2CO_3 decomposition [28,29]. The hydrolysis of Na_2CO_3 was shown to proceed at above 400 °C [29,30]. Experimentally, $NaHCO_3$ decomposition according to reaction (3-reverse) proceeded at above 80 °C and attained completion in the range 100–180 °C [18,31–33]. In a closed vessel at 100 °C, it yielded $Na_2CO_3{\cdot}3NaHCO_3$ [32].

This paper examines the thermodynamic and kinetics of the pertinent reactions for three selected Na-based closed-material cycles for capturing CO_2 from air. Thermogravimetric runs are carried at low CO_2 concentrations (500 ppm[1]), aiming to simulate the capture of CO_2 from air. Comparison among these cycles in terms of equilibrium compositions, energy requirements, and reaction extents is discussed.

2. Thermodynamic analysis

2.1. Equilibrium compositions

Thermochemical equilibrium computations based on Gibbs energy minimization were carried out using Outokumpu HSC Chemistry code [34,35]. Species whose mole fraction was less than 10^{-5} have been omitted from the figures. The equilibrium composition for NaOH(s) and air containing 500 ppm of CO_2 (stoichiometry: 1 kmol NaOH + 1 kmol CO_2 + 420 kmol O_2 + 1575 kmol N_2; corresponding to a NaOH:CO_2 molar ratio of 1) is shown in Fig. 1 as a function of temperature. Both carbonation reactions (1) and (2) are thermodynamically favorable at ambient temperature, yielding Na_2CO_3 and $NaHCO_3$ with a solid molar fraction of 27 and 55%, respectively, in addition to 15% of sodium carbonate monohydrate ($Na_2CO_3{\cdot}H_2O$) and 3% of trona ($Na_3CO_3HCO_3{\cdot}2H_2O$). With increasing temperature, $Na_2CO_3{\cdot}H_2O$ dehydrates and $NaHCO_3$ decomposes into Na_2CO_3 according to reaction (3-reverse). At 312 °C, no other Na-based compound other than Na_2CO_3 is present. At above 400 °C, Na_2CO_3 is converted in the presence of water vapor into NaOH according to reaction (6), as was experimentally shown [29,30]. At above 1200 °C, NaOH is the only solid species in equilibrium.

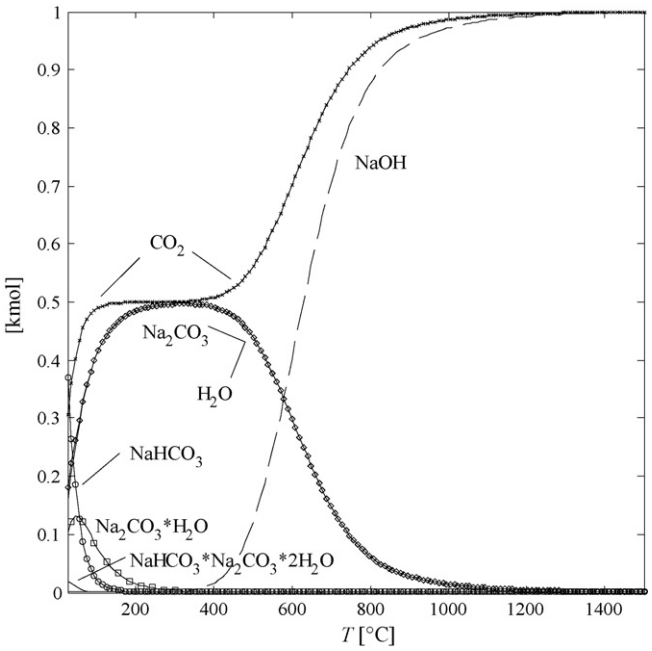

Fig. 1. Equilibrium composition of NaOH(s) + air (stoichiometry: 1 kmol NaOH + 1 kmol CO_2 + 420 kmol O_2 + 1575 kmol N_2) vs. temperature at 1 bar. *Note*: the curves for N_2 and O_2 are not shown; the curves for Na_2CO_3 and H_2O are congruent.

The equilibrium composition for Na_2CO_3(s), H_2O, and air containing 500 ppm of CO_2 (stoichiometry: 1 kmol Na_2CO_3 + 1 kmol H_2O + 1 kmol CO_2 + 420 kmol O_2 + 1575 kmol N_2) is shown in Fig. 2 as a function of temperature. At ambient temperature, the solid species at equilibrium are $NaHCO_3$, Na_2CO_3, $Na_2CO_3{\cdot}H_2O$, and trona, with a solid molar fraction of 63, 23, 12, and 2%, respectively. As in the previous case, with increasing temperature the hydrated compounds lose water and $NaHCO_3$ decomposes into Na_2CO_3 (reaction 3-reverse). At 312 °C, Na_2CO_3 is the only Na-based compound in equilibrium. The hydrolysis of Na_2CO_3 into NaOH is completed at around 1200 °C (reaction (6)). Note that Wegscheider's salt ($3NaHCO_3{\cdot}Na_2CO_3$) has been excluded from consideration. It has been observed to be an intermediate compound of reaction (3) [36]. However, as it will be explained

[1] Assumption: predicted 500 ppm CO_2 concentration in the ambient air by the time the proposed technology would be commercially available for application.

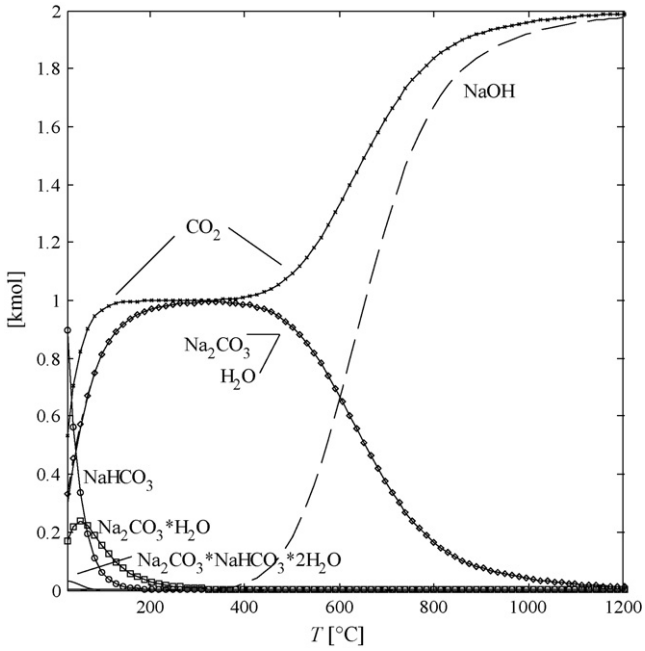

Fig. 2. Equilibrium composition of $Na_2CO_3(s) + air + H_2O$ (stoichiometry: 1 kmol NaOH + 1 kmol CO_2 + 1 kmol H_2O + 420 kmol O_2 + 1575 kmol N_2) vs. temperature at 1 bar. *Note*: the curves for N_2 and O_2 are not shown; the curves for Na_2CO_3 and H_2O are congruent.

in the thermogravimetric analysis that follows, Wegscheider's salt was not detected by XRD among the products.

The equilibrium composition for 1 kmol $NaHCO_3$ as a function of temperature is shown in Fig. 3. As previously reported, $NaHCO_3$ decomposition according to reaction (3-reverse) proceeds at above 80 °C and reaches completion in the range 100–180 °C [18,31–33]. The reaction is thermodynamically favorable in the range 25–400 °C. The equilibrium composition is similar to the previous two cases, but the absence of air (large

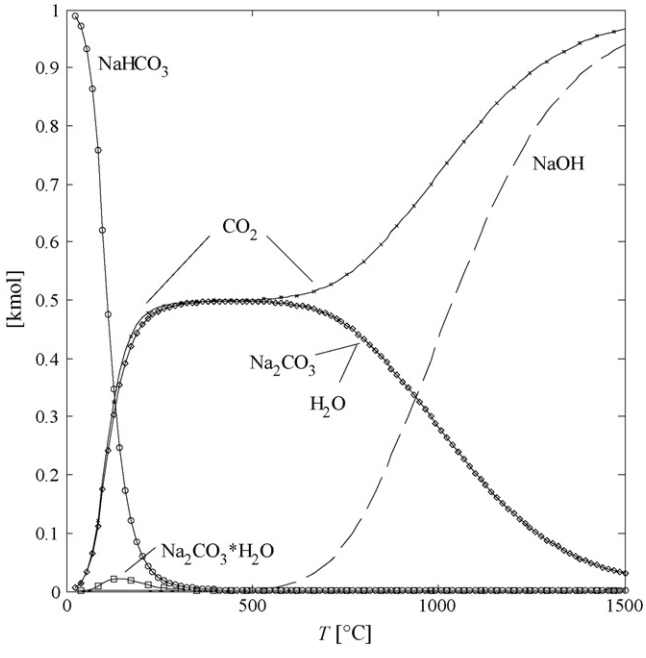

Fig. 3. Equilibrium composition of 1 kmol $NaHCO_3$ (s) vs. temperature at 1 bar.

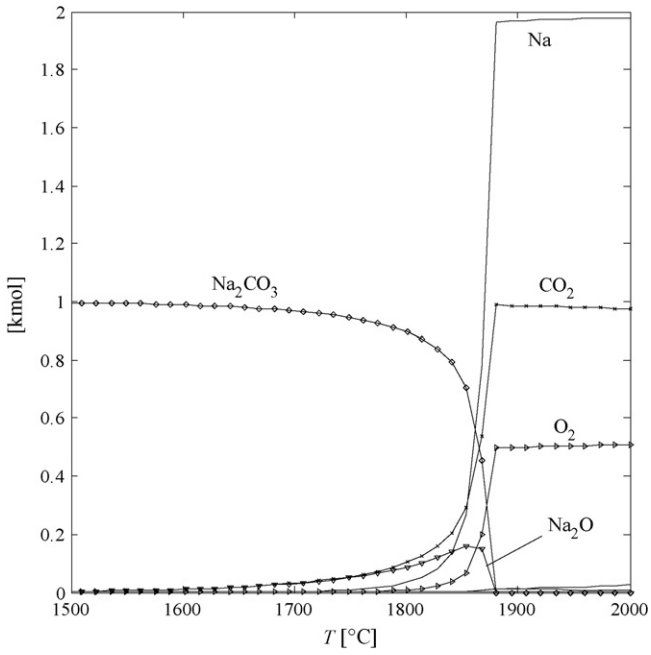

Fig. 4. Equilibrium composition of Na_2CO_3(s) vs. temperature at 1 bar.

amounts of N_2 and O_2 acting as inert gases) displaces the equilibrium to higher temperatures as expected for solid decomposition processes.

The equilibrium composition for 1 kmol Na_2CO_3 as a function of temperature is shown in Fig. 4. Na_2CO_3 starts to decompose at above 1600 °C and proceeds in two steps, firstly to Na_2O according reaction (4), and finally to Na(g) at above 1850 °C, as previously suggested [26]. The second step is believed to proceed at high rates [37]. Above 1900 °C, the equilibrium composition consisted of a single gas phase containing Na, O_2, and CO_2.

3. Thermochemical cycles

Three closed-materials thermochemical cycles are considered. The selection of the operating temperatures of the carbonation and decarbonation steps is based on the results of the chemical equilibrium computations (see Section 2) and thermogravimetric analyses (see Section 4).

3.1. Thermochemical Cycle 1

The closed-material Cycle 1 is depicted in Fig. 5 and encompasses 4 main chemical reactors. Atmospheric air, containing 500 ppm of CO_2, is injected at 25 °C along with NaOH into the reactor I (carbonator), where reaction (2) takes place at ambient temperature. The solid product $NaHCO_3$ is fed to reactor II, where undergoes thermal decomposition at 200 °C to Na_2CO_3, CO_2 and H_2O according to reaction (3). The products of the decomposition undergo natural phase separation (not shown in the schematic). Pure CO_2, after being cooled to ambient temperature, is delivered to the storage site. Na_2CO_3 is directed to a heat exchanger III for pre-heating to 590 °C before entering the reactor IV. In the reactor IV, Na_2CO_3 thermally decomposes at

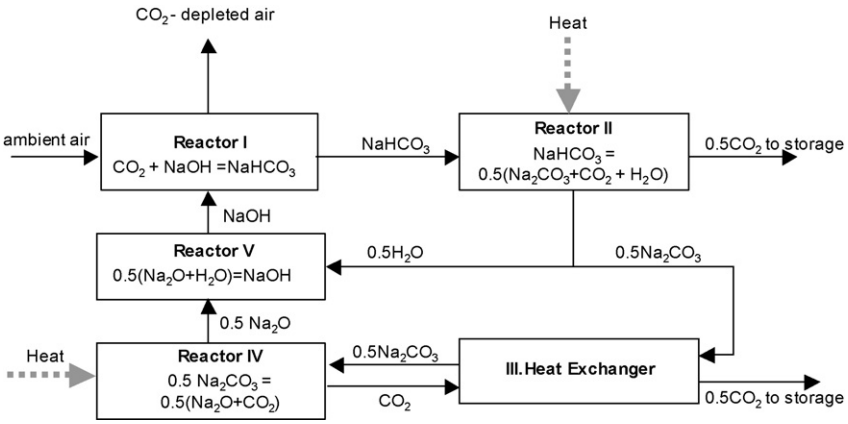

Fig. 5. Schematic of the thermochemical Cycle 1 for CO_2 capture from air.

1400 °C to Na_2O and CO_2 according to reaction (4). CO_2, after being cooled in the heat exchanger III to 240 °C, is quenched to ambient temperature and delivered to the storage site. Na_2O is directed to the reactor V where it reacts with H_2O coming from reactor II to form of NaOH at 727 °C. High-temperature process heat is supplied to the endothermic reactions (3) and (4).

3.2. Thermochemical Cycle 2

The closed-material Cycle 2 is depicted in Fig. 6. It features the same first two steps of Cycle 1, but reactions (4) and (5) are replaced by the single reaction (1-reverse). Na_2CO_3, after leaving reactor II, is directed to the heat exchanger, where undergoes preheating to 360 °C before being fed to reactor III. In reactor III, it is steam-hydrolyzed at 700 °C to NaOH and CO_2 according to the reaction (1-reverse). The second portion of CO_2, after being cooled in the heat exchanger IV to 240 °C, is quenched to ambient temperature and delivered to the storage site. High-temperature process heat is supplied for the endothermic reaction (3-reverse) and reaction (1-reverse).

3.3. Thermochemical Cycle 3

The closed-material Cycle 3 is depicted in Fig. 7. It is based on the reversible reaction (3). Atmospheric air, containing 500 ppm of CO_2, is injected at 25 °C into the heat exchanger III where it undergoes preheating to 44 °C by the CO_2-depleted air flow. Afterwards, it is delivered to reactor I, where it reacts with Na_2CO_3 in presence of water at 50 °C to form $NaHCO_3$(s). $NaHCO_3$ is preheated to 67 °C and then fed to reactor II, where it is thermally decomposed to Na_2CO_3, H_2O and CO_2 at 200 °C. The products of the decomposition undergo a natural phase separation (not shown in the schematic). Na_2CO_3 and H_2O are recycled to reactor I, while pure CO_2, after being cooled in the heat exchanger IV to 90 °C, is delivered to the storage site. Process heat is supplied to the endothermic reaction (3-reverse); the exothermic reaction (3) is used for heating the reactants to 50 °C.

3.4. Energy balances

The baseline design assumes the capture of 1 mol/s of CO_2. Na_2CO_3, H_2O, and CO_2 undergo a natural phase separation without input of work. All heat exchangers are ideal, all substances are pure, and all reactions achieve chemical equilibrium. Parasitic energy consumption, e.g. solids transport and air pumping, has been omitted from consideration. In practice, pumping work, heat transfer irreversibilities, and material impurities result in a reduction of the process efficiency. The use of carrier gas required for transporting CO_2 out of the reactor during the decomposition processes has been neglected. Baseline operational parameters and mass/energy balances are summarized in Table 1. The energy balances of Cycles 1, 2, and 3 were carried out based on the enthalpy difference of mass flow in and out of each module. The total energy requirements for Cycles 1, 2,

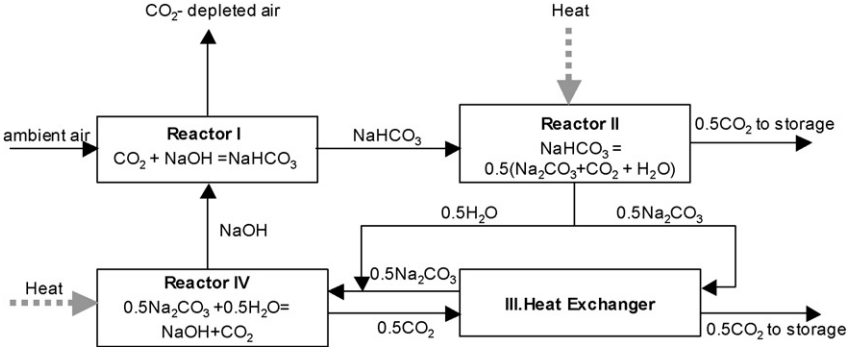

Fig. 6. Schematic of the thermochemical Cycle 2 for CO_2 capture from air.

Table 1
Baseline operational parameters and mass/energy balances for the capture of 1 mol/s of CO_2 from air

Cycle	Module Nr		Temperature (°C)	Mass flow (kg/h)	Power (kW)
1	I. Carbonator	NaOH (s) in	25	144	
		Polluted air/CO_2 in	25	208568.4	
		$NaHCO_3$(s) out	25	604.9	
		CO_2-dep. air/out	25	208409.9	
		Reaction (2)	25		−131.5
	II. Decarbonator	$NaHCO_3$(s) in	25	604.9	
		H_2O out	200	32.4	
		CO_2 out	200	79.2	
		Na_2CO_3 (s) out	200	190.8	
		Reaction (3)	200		85.1
	III. Heat exchanger	CO_2 in	1400	79.2	
		Na_2CO_3 (s) in	200	190.8	
		CO_2 out	240	79.2	
		Na_2CO_3 (s) out	590	190.8	
					46.7
	IV. Decarbonator	Na_2CO_3 (s) in	590	190.8	
		Na_2O (g) out	1400	111.6	
		CO_2 out	1400	79.2	
		Reaction (4)	1400		396.1
	V. Hydrolyser	Na_2O (g) in	1400	111.6	
		H_2O in	200	32.4	
		NaOH (s) out	727	144	
		Reaction (5)	727		−268.09
	Loss by cooling				−81.58
	Total energy requirement for endothermic reactions				481.2
2	I. Carbonator	NaOH (s) in	25	144	
		Polluted air/CO_2 in	25	208568.4	
		$NaHCO_3$(s) out	25	604.9	
		CO_2-dep. air/out	25	208409.9	
		Reaction (2)	25		−131.5
	II. Decarbonator	$NaHCO_3$(s) in	25	604.9	
		H_2O out	200	32.4	
		CO_2 out	200	79.2	
		Na_2CO_3 (s) out	200	190.8	
		Reaction (3)	200		85.1
	III. Heat exchanger	CO_2 in	700	79.2	
		Na_2CO_3 (s) in	200	190.8	
		CO_2 out	240	79.2	
		Na_2CO_3 (s) out	360	190.8	27.5
	IV. Hydrolyser	Na_2CO_3 (s) in	360	190.8	
		H_2O in	200	32.4	
		NaOH (s) out	700	144	
		CO_2 out	700	79.2	
		Reaction (2-reverse)			128
	Loss by cooling				−81.58
	Total energy requirement for endothermic reactions				213.1
3	I. Carbonator	Na_2CO_3 (s) in	25	381.6	
		Polluted air/CO_2 in	43.8	208568.4	
		H_2O in	25	64.9	
		$NaHCO_3$(s) out	50	604.9	
		CO_2-dep. air/out	50	208409.9	
		Reaction (4-reverse)	50		232.3
	II. Decarbonator	$NaHCO_3$(s) in	66.7	604.9	
		H_2O out	200	64.9	
		CO_2 out	200	158.4	
		Na_2CO_3 (s) out	200	381.6	
		Reaction (3)	200		157.81
	III. Heat Exchanger	Polluted air/CO_2 in	25	208568.4	
		CO_2-dep. air/in	50	208409.9	
		Polluted air/CO_2 out	43.8	208568.4	
		CO_2-dep. air/out	30	208409.9	190.8
	IV. Heat Exchanger	CO_2 in	200	158.4	
		$NaHCO_3$(s) in	50	604.9	
		CO_2 out	90	158.4	
		$NaHCO_3$(s) out	66.7	604.9	14.08
	Loss by cooling				−25.5
	Total energy requirement for endothermic reactions				390.1

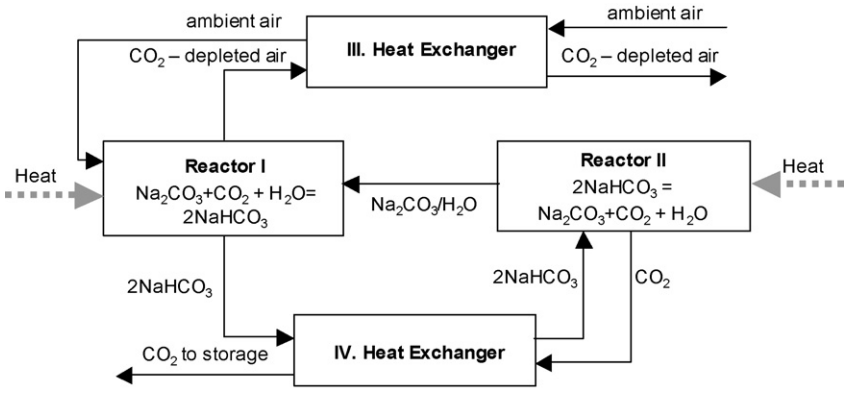

Fig. 7. Schematic of the thermochemical Cycle 3 for CO_2 capture from air.

and 3, i.e. the sum of the enthalpy changes of the endothermic reactions, are 481.2, 213.1, and 390.1 kW/mol/s CO_2 captured, respectively.

4. Thermogravimetric analysis

4.1. Experimental set-up

Experimentation was carried out in a thermogravimeter system (TG, Netzsch STA 409 CD) equipped with two furnaces: a conventional high-temperature electric furnace with a maximum working temperature of 1550 °C and suitable for reactive atmospheres having a dew point below room temperature, and a special electric furnace with a maximum working temperature of 1250 °C and suitable for reactive atmospheres containing up to 100% steam at 1 bar total pressure. The reactive gas enters the furnace chamber and flows upwards past a thin layer of solid reactant mounted on a 17 mm-diameter Al_2O_3 crucible. The crucible is equipped with a thermocouple of type S that provides direct temperature measurement of the sample. The mass flow rates of the reactive gas are adjusted by electronic flow controllers for Ar, CO_2, and water (Vögtlin Q-FLOW, Bronkhorst LIQUI-FLOW). Product gas composition at the TG exit is analyzed every 60 s by gas chromatography (2 channel Varian Micro GC, equipped with Molsieve-5A and Poraplot-U columns). For the dynamic runs, the sample was heated at a rate of 20 K/min to the desired temperature while being subjected to a constant reaction gas flow. For the isothermal runs, the sample was heated to the desired temperature under Ar, kept for 20 min at isothermal conditions to ensure stabilization, and then subjected to a constant reaction gas flow under isothermal conditions. Typically, 60 mg of powder were placed on the sample holder. The specific surface areas of NaOH and $NaHCO_3$ samples, determined by BET (Micromeritics, TriStar), were 3.54 and 10.07 m^2/g, respectively. Synthetic air containing 500 ppm of CO_2 mixed with Ar at a total flow rate of 180 ml/min was constantly supplied to the furnace during the carbonation runs.

The reaction extent X for the carbonation of NaOH is defined as:

$$X_{\mathrm{NaOH}} = 1 - \frac{n_{\mathrm{NaOH}}(t)}{n_{\mathrm{NaOH},0}} \quad (7)$$

where $n_{\mathrm{NaOH},0}$ and $n_{\mathrm{NaOH}}(t)$ are the number of moles of NaOH initially and after reaction time t, respectively. The extent of other reactions is defined analogously.

4.2. Experimental results

Fig. 8 shows the temperature, the relative weight increase of NaOH (measured by TG), and the CO_2 concentration at the exit (measured by GC) for the carbonation of NaOH during an isothermal TG run at 25 °C and atmospheric pressure. The NaOH carbonation reaction, applied in Cycles 1 and 2, occurs according to reaction (2). No other compounds are formed except $NaHCO_3$, as it will be proved in the analysis that follows. The total amount of CO_2 captured after 240 min was 1.2×10^{-4} mol when based on the integration of the CO_2 curve recorded by GC [38], and 1.1×10^{-4} mol when based on the mass increase recorded by TG. After 240 min of the experiment, the reaction extent amounts to $X_{\mathrm{NaOH}} = 0.09$.

Fig. 9 shows the temperature, the relative weight increase of Na_2CO_3, and the CO_2 concentration at the exit for the

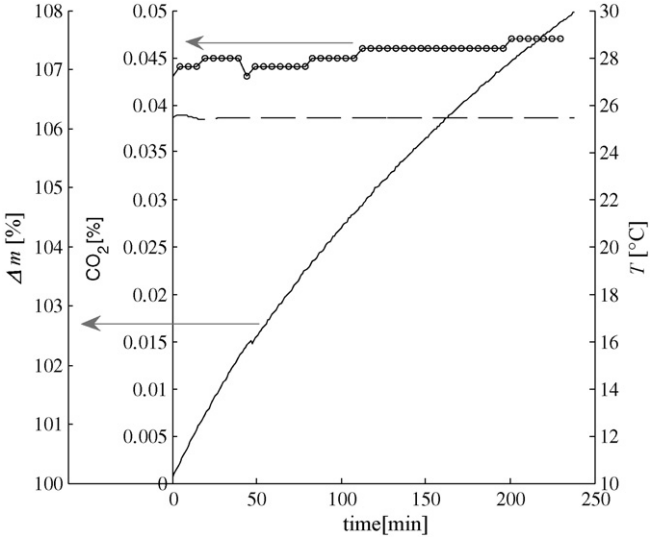

Fig. 8. Relative weight increase of NaOH and CO_2 concentration at the exit during an isothermal TG run for the NaOH carbonation with synthetic air containing 500 ppm at 25 °C and atmospheric pressure.

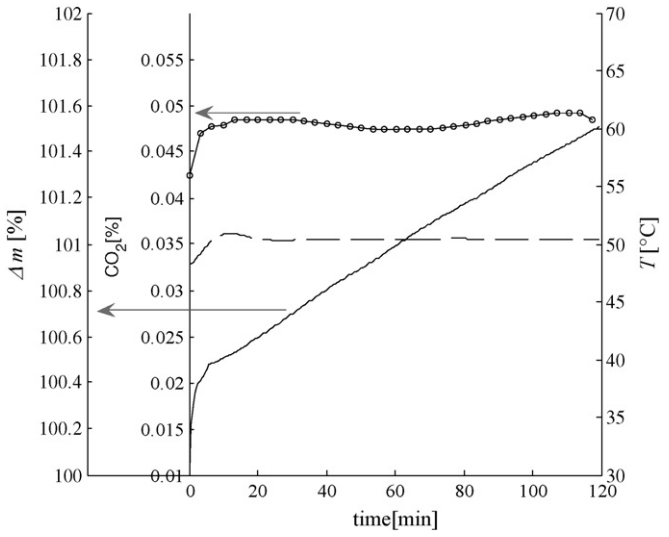

Fig. 9. Relative weight increase of Na_2CO_3 and CO_2 concentration at the exit during an isothermal TG run for the Na_2CO_3 carbonation with synthetic air saturated with water at 50 °C and atmospheric pressure.

carbonation of Na_2CO_3 during an isothermal TG run with synthetic air saturated with water at 50 °C and atmospheric pressure. The water concentration is maintained at 6.2% by saturating the synthetic air flow with a humidifier at 50 °C. The Na_2CO_3 carbonation reaction, applied in Cycle 3, occurs according to reaction (3). The reaction extent reaches only 3.5% after 120 min. The total amount of CO_2 captured after 120 min was 2.38×10^{-5} mol when based on the integration of the CO_2 curve recorded by GC, and 2.02×10^{-5} mol when based on the mass increase recorded by the TG. No detectable carbonation of Na_2CO_3 was observed in the temperature range 40–70 °C with water concentration of 1.6%. Fig. 10 shows the XRD patterns of the products of the TG run of Fig. 9. Trona or Wegscheider's salt were not detected among the products. Mass balance further supports that the formation of these slats was negligible.

Fig. 11 shows the relative weight decrease of $NaHCO_3$, and the CO_2 concentration at the exit for the decomposition of

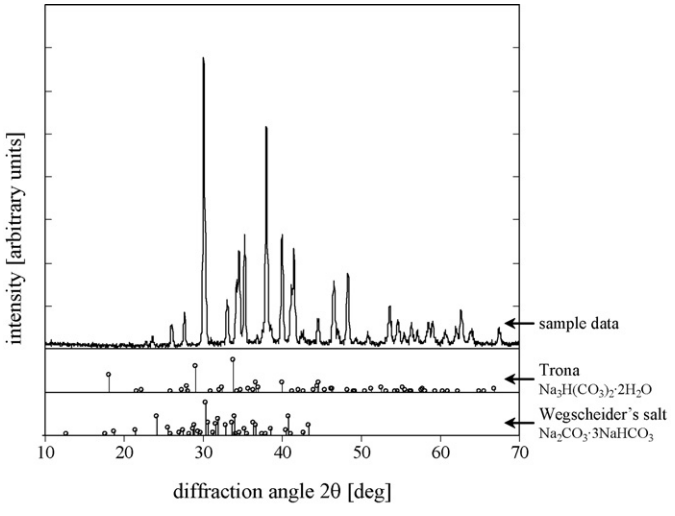

Fig. 10. XRD patterns of the products of the carbonation of Na_2CO_3 (sample data; Fig. 9), and of trona and Wegscheider's salts.

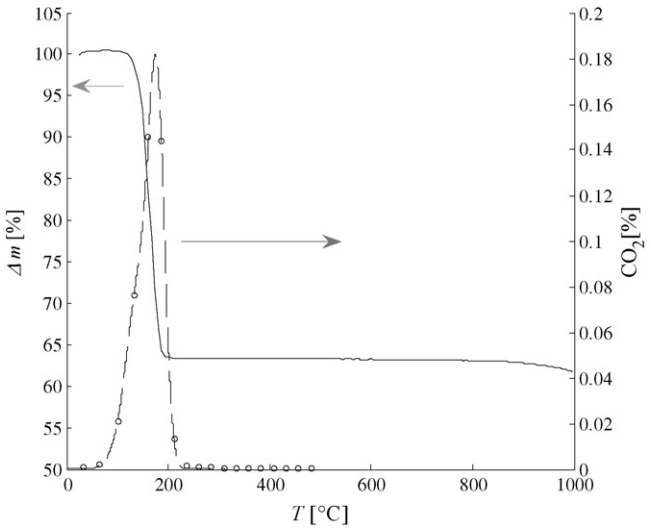

Fig. 11. Relative weight decrease of $NaHCO_3$, and CO_2 concentration at the exit during a dynamic TG run for the $NaHCO_3$ decomposition in Ar.

$NaHCO_3$ during a dynamic TG run in Ar in the 25–530 °C range. Full decomposition ($\Delta m = 99.97\%$) of $NaHCO_3$ was achieved in 3 min in the temperature range from 90 to 200 °C. The $NaHCO_3$ decomposition reaction, applied in all three cycles, occurs according to reaction (3-reverse). No NaOH is reformed. This result is consistent with previously reported data [32,33]. The total amount of CO_2 released was 3.99×10^{-4} mol when based on the integration of the CO_2 curve recorded by GC and 3.84×10^{-4} mol when based on the mass decrease recorded by TG.

Fig. 12 shows a combined carbonation/decomposition run that was performed for the purpose of elucidating the NaOH–CO_2 interaction. The carbonation of NaOH with synthetic air was firstly studied in an isothermal TG run at 25 °C

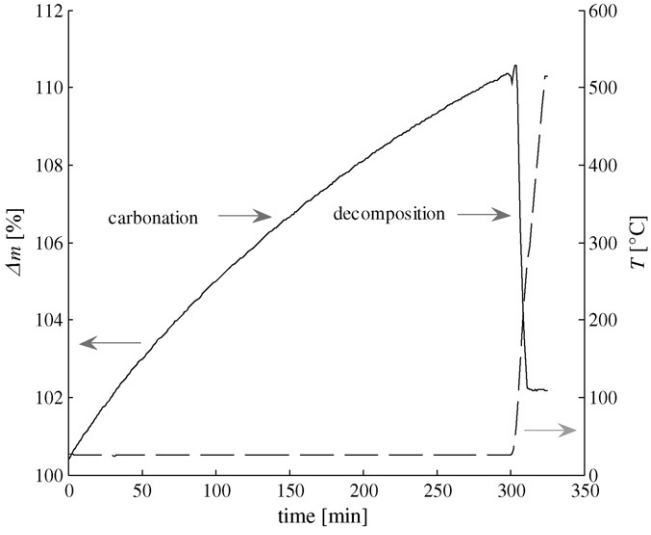

Fig. 12. Relative weight increase and temperature during a combined carbonation-decomposition run. The carbonation of NaOH with synthetic air was firstly studied in an isothermal TG run at 25 °C during 300 min. Afterwards, synthetic air flow was stopped and the decomposition of the formed products was studied in an dynamic TG run at a heating rate of 20 °C/min.

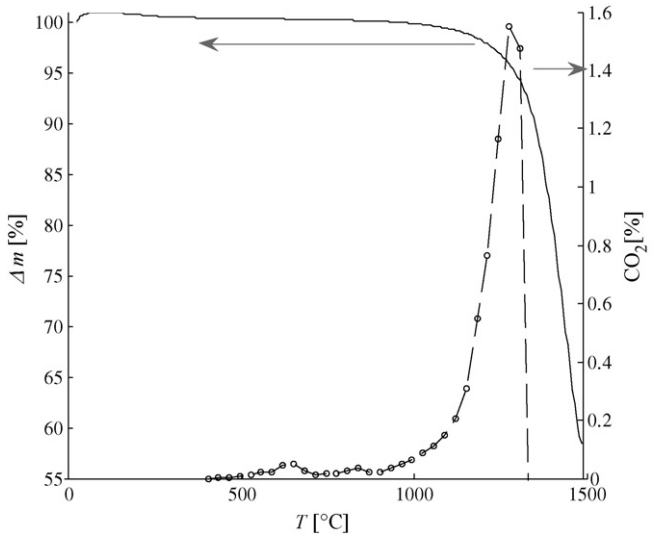

Fig. 13. Relative weight decrease of Na_2CO_3, and CO_2 concentration at the exit during a dynamic TG run for the Na_2CO_3 decomposition in Ar.

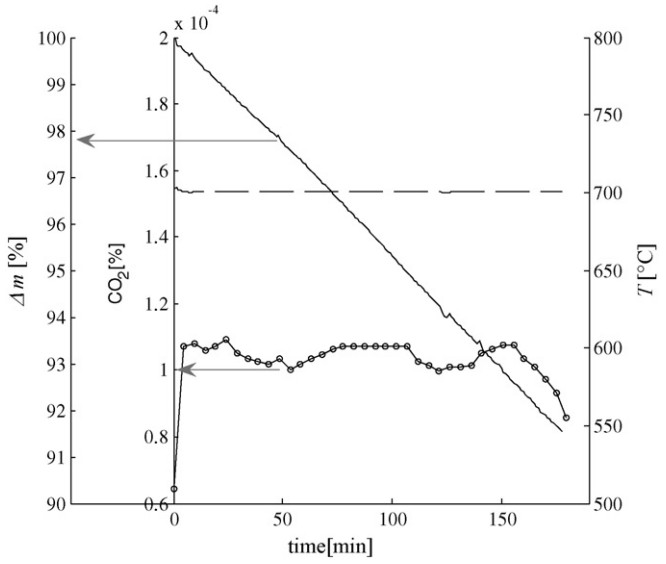

Fig. 14. Relative weight decrease of Na_2CO_3 and CO_2 concentration at the exit during an isothermal TG run for Na_2CO_3 hydrolysis with 50% of water vapor in Ar at 700 °C and atmospheric pressure.

during 300 min. Afterwards, synthetic air flow was stopped and the decomposition of the formed products was studied in an dynamic TG run at a heating rate of 20 °C/min. After 12 min, at 300 °C, the decarbonation was completed, as attested by no change in the sample weight. Assuming that $NaHCO_3$ is the only species formed after the carbonation process according to reaction (2), mass balance of the carbonation part of the run yields a reaction extent is 9.43% after 5 h, which corresponds to a yield of 13.1 mg of $NaHCO_3$. Mass balance on the decarbonation part of the run yields 12.99 mg of $NaHCO_3$. Thus, $NaHCO_3$ is the only species formed during NaOH carbonation under the given conditions. The decomposition of $NaHCO_3$ proceeded according to reaction (3-reverse) to form Na_2CO_3 (SSA[2] of 0.177 m^2/g), CO_2 and H_2O.

The decomposition of Na_2CO_3 was subsequently studied to identify possible routes for NaOH regeneration. Fig. 13 shows the relative weight decrease of Na_2CO_3, and the CO_2 concentration at the exit for the decomposition of Na_2CO_3 during a dynamic TG run in Ar in the 25–1400 °C range. An Al_2O_3 cup-crucible was used as sample holder to prevent the loss of Na_2CO_3 and Na_2O during melting. A 41.8% relative mass loss occurred in 15 min at 1000–1400 °C due to the release of CO_2 and the conversion of Na_2CO_3 to Na_2O [39,40]. The total amount of CO_2 released after 15 min of reaction was 5.98×10^{-4} mol when based on the integration of the CO_2 curve, and 5.83×10^{-4} mol when based on the mass decrease. Thus, the reaction proceeds to completion according to reaction (4), yielding Na_2O(l) – which solidifies during cooling – and CO_2, as observed earlier [23,25–27].

Finally, a direct way to recover NaOH from Na_2CO_3 would be according to the reaction (1-reverse), applied in Cycle 2. Fig. 14 shows relative weight decrease of Na_2CO_3 and CO_2 concentration at the exit for the hydrolysis of Na_2CO_3 with a 146 ml/min flow of 50% H_2O in Ar during an isothermal TG run at 700 °C and atmospheric pressure. A 8.7% relative mass loss occurred after 3 h, corresponding to a reaction extent of 35.2%. The product of the reaction is NaOH(l), which solidifies during cooling. The total amount of CO_2 released after 180 min was 1.87×10^{-4} mol when based on the integration of the CO_2 curve recorder by GC, and 2.07×10^{-4} mol when based on the mass decrease recorded by TG. The inconsistency in the mass balance is attributed to partial gasification of Na_2CO_3 during heating. No reaction was observed for similar runs at temperatures below 650 °C.

5. Discussion and conclusions

Three closed-material thermochemical cycles for CO_2 capture from air were examined. Cycles 1 and 2 are based on the carbonation of NaOH to $NaHCO_3$, whose reaction extent with 500 ppm CO_2 in air at 25 °C reached 9% after 4 h. Complete thermal decomposition of $NaHCO_3$ into Na_2CO_3, CO_2, and H_2O was achieved after 3 min in the 90–200 °C range, while complete thermal decomposition of Na_2CO_3 into Na_2O and CO_2 was achieved after 15 min in the 1000–1400 °C range. Finally, NaOH is regenerated by steam-hydrolysis of Na_2O. Alternatively, Cycle 2 applies the direct hydrolysis of Na_2CO_3 without intermediate step, whose reaction extent reached 35.2% after 3 h with 50% H_2O in Ar at 700 °C. Cycle 3 is based on the reversible carbonation of Na_2CO_3 to form $NaHCO_3$, whose reaction extent reached only 3.5% after 2 h with water-saturated synthetic air at 50 °C and atmospheric pressure (6.2% water concentration). The slow reaction rate of the carbonation steps for all cycles considered impedes the application of Na-based sorbents.

A preliminary evaluation of the dimensions of the carbonator is carried out to estimate the feasibility of the CO_2 absorption process from air using Na-based sorbents and to compare it with the previously suggested cycles using Ca-based sorbents [1,2]. In Cycle 3, about 2.6% of Na_2CO_3 carbonates into $NaHCO_3$

[2] Determined by BET, Micromeritics, TriStar.

after 100 min (Fig. 9). The required mass flow rate of the sorbent fed to the absorber for capturing 1 mol/s of CO_2 would be then 4.07 kg/s of Na_2CO_3. Considering that this reaction extent is reached after 100 min, the inventory of Na_2CO_3 in the carbonator would amount to 24 tonnes, making the process technically and economically unfeasible. Similarly, for Cycles 1 and 2, the inventory of NaOH in the carbonator would amount to 3.4 tonnes. In contrast, Ca-based sorbents are advantageous because of their higher conversion rates and yields, thus lowering the inventory of solids, but at the expense of higher required carbonation temperatures. For example, 40% of $Ca(OH)_2$ and 80% of CaO (in presence of water vapor) carbonates to $CaCO_3$ after 100 min at 450 °C [2]. In this case, the mass flow rates of $Ca(OH)_2$ and CaO for capturing at a rate of 1 mol/s of CO_2 would be 0.2 and 0.07 kg/s (with 19.6 kg/s of water vapor), respectively, and the inventory of solids $Ca(OH)_2$ and CaO in the absorber would be 1202 and 425 kg, respectively.

References

[1] V. Nikulshina, D. Hirsch, M. Mazzotti, A. Steinfeld, CO_2 capture from air and co-production of H_2 via the $Ca(OH)_2$–$CaCO_3$ cycle using concentrated solar power—thermodynamic analysis, Energy 31 (2006) 1379–1389.

[2] V. Nikulshina, E. Gálvez, A. Steinfeld, Kinetic analysis of the carbonation reactions for the capture of CO2 from air via the $Ca(OH)_2$–$CaCO_3$–CaO solar thermochemical cycle, Chem. Eng. J. 129 (2007) 75–83.

[3] R. Baciocchi, G. Storti, M. Mazzotti, Process design and energy requirements for the capture of carbon dioxide from air, Chem. Eng. Process. 45 (2006) 1047–1058.

[4] M. Zanfir, A. Gavriilidis, Ch. Wille, V. Hessel, Carbon dioxide absorbtion in a falling film microstructured reactor: experiments and modeling, Ind. Eng. Chem. Res. 44 (2005) 1742–1751.

[5] R. Pohorecki, W. Moniuk, Kinetics of reaction between carbon dioxide and hydroxyl ions in aqueous electrolyte solutions, Chem. Eng. Sci. 43 (1988) 1677–1684.

[6] J. Ager, C. Howard, Rate coefficient for the gas phase reaction of NaOH with CO_2, Geophys. Res. J. 92 (1987) 6675–6678.

[7] D. Herskowits, V. Herskowits, K. Stephan, A. Tamir, Characterization of a two-phase impinging jet absorber-II. Absorption with chemical reaction of CO_2 in NaOH solutions, Chem. Eng. Sci. 45 (1990) 1281–1287.

[8] D. Darmana, N. Deen, J. Kuipers, Detailed modelling of hydrodynamics, mass transfer and chemical reactions in a bubble column using a discrete bubble model, Chem. Eng. Sci. 60 (2005) 3383–3404.

[9] M. Taghizadeh, C. Jallut, M. Tayakout-Fayolle, J. Lieto, Non-isothermal gas–liquid absorption with chemical reaction studies. Temperature measurements of a spherical laminar film surface and comparison with a model for the CO_2/NaOH system, Chem. Eng. J. 82 (2001) 143–148.

[10] F. Takemura, Y. Matsumoto, Dissolution rate of spherical carbon dioxide bubbles in strong alkaline solutions, Chem. Eng. Sci. 55 (2000) 3907–3917.

[11] A. Sprygin, L. Khoroshavin, V. Ust'yantsev, A. Purgin, V. Mar'evich, Y. Filin, N. Ivanov, A. Tikhomirov, Mechanism of hardening of refractory concrete composites containing water glass with CO_2 purging, Ogneupory 1 (1982), p.38.

[12] C. Fleischer, S. Becker, G. Eigenberger, Detailed modelling of the chemisorption of CO_2 into NaOH in a bubble column, Chem. Eng. Sci. 51 (1996) 1715–1724.

[13] B. Banadda, M. Prost, S. Ismaily, R. Bressat, M. Otterbein, Validation of the gas-lift capillary bubble column as a simulation device for a reactor by the study of CO_2 absorption in Na_2CO_3/$NaHCO_3$ solutions, Chem. Eng. Process. 33 (1994) 55–59.

[14] D. Roberts, P. Danckwerts, Kinetics of CO_2 absorption in alkaline solutions-ITransient absorption rates and catalysis by arsenite, Chem. Eng. Sci. 17 (1962) 961–969.

[15] A. Meisenz, C. Jim Lim, P. Tontiwachwuthikul, CO_2 absorption by NaOH, monoethanolamine and 2-amino-2-methyl-l-propanol solutions in a packed column, Chem. Eng. Sci. 47 (1992) 381–390.

[16] S. Ebrahimi, C. Picioreanua, R. Kleerebezema, J. Heijnena, M. van Loosdrechta, Rate-based modelling of SO_2 absorption into aqueous $NaHCO_3$/Na_2CO_3 solutions accompanied by the desorption of CO_2, Chem. Eng. Sci. 58 (2003) 3589–3600.

[17] Stolaroff, D. Keith, G. Lowry, Contactor energy requirements for capturing CO_2 from ambient air using NaOH determined in a pilot-scale prototype system, in: AGU Fall Meeting, San Francisco, CA, December 5–9, 2005.

[18] Sodium carbonates, in: Wiley–Ullman's Encyclopedia of Industrial Chemistry, Wiley-VCH Verlag GmbH & Co., Weinheim, 2005.

[19] The Merck index, in: Encyclopedia of Chemicals, Drugs and Biologicals, Merck and Co, Inc., Budavari, NJ, 1989, p. 1357.

[20] P. Patnaik, Handbook of Inorganic Chemicals, McGraw-Hill, 2003.

[21] B.S. Ya Liang, Carbon dioxide capture from flue gas using regenerable sodium-based sorbents, Ph.D. Thesis, Tsinghua University, 2003.

[22] A. Cents, D. Brilman, G. Versteeg, CO_2 absorption in carbonate/bicarbonate solutions: the Danckwerts-criterion revisited, Chem. Eng. Sci. 60 (2005) 5830–5835.

[23] V. Babushok, K. McNesby, A. Miziolek, R. Skaggs, Modeling of synergistic effects in flame inhibition by 2-H heptafluoropropane blended with sodium bicarbonate, Combust. Flame 133 (2003) 2001–2205.

[24] A. Newkirk, I. Aliferis, Drying and decomposition of sodium carbonate, Anal. Chem. 3 (1958) 982–984.

[25] T. Wigmans, J. van Doorn, J. Moulijn, Temperature-programmed desorption study of Na_2CO_3-containing activated carbon, Fuel 62 (1983) 190–195.

[26] Mass spectrometric study of volatile components in mould powders, Andrei Chilov. Doctoral Thesis, Helsinki University of Technology, 2005.

[27] J. Kim, Y. Lee, H. Lee, Decomposition of Na_2CO_3 by interaction with SiO_2 in mold flux of steel continuous casting, ISIJ Int. 41 (2001) 116–123.

[28] M. Alonso-Porta, R. Kumar, Use of NASICON/Na_2CO_3 system for measuring CO_2, Sen. Actuators B 71 (2000) 173–178.

[29] V. Zamansky, P. Maly, M. Sheldon, W. Seeker, B. Folsom, Second generation advanced reburning for high efficiency NOx control, Energy and Environmental Research Corporation.U.S. Department of Energy's Federal Energy Technology Center No. DE-AC22-95PC95251, 1998.

[30] C. Kröger, E. Fingas, Z. Anorg. Allgem. Chem. 212 (1933) 257–268.

[31] Y. Wu, S. Shih, Intrinsic kinetics of the thermal decomposition of sodium carbonate, Thermochem. Acta 223 (1993) 177–186.

[32] E. Barrall, L. Rogers, Differential thermal analysis of the decomposition of sodium bicarbonate and its simple double salts, J. Inorg. Nucl. Chem. 28 (1966) 41–51.

[33] P. Heda, D. Dollimore, K. Alexander, D. Chen, E. Law, P. Bicknell, A method of assessing solid state reactivity illustrated by thermal decomposition experiments on sodium bicarbonate, Thermochim. Acta 255 (1995) 255–272.

[34] A. Roine, Outokumpu HSC Chemistry for Windows, Outokumpu Research, Pori, Finland, 1997.

[35] Y. Lwin, Chemical equilibrium by Gibbs energy minimization on spreadsheets, Int. J. Eng. Ed. 16 4 (2000) 335–339.

[36] Y. Liang, Carbon dioxide capture using dry sodium-based sorbents, Energ Fuel 18 (2004) 569–575.

[37] K. Motzfeldt, Thermal decomposition of sodium carbonate by the effusion method, J. Phys. Chem. 59 (1955) 139.

[38] Matlab R14, The MathWorks Inc., Boston, MA, 2005.

[39] Sodium carbonate, in: Material Safety Data. MSDS S3242, Mallinckrodt Baker, Inc., 1998.

[40] R. Lewis, Sodium carbonate, in: Sax's Dangerous Properties of Industrial Materials 9, Van Nostrand Reihold, NY, 1996, p. 2952.